

## Predicting space climate change

L. Barnard,<sup>1</sup> M. Lockwood,<sup>1,2</sup> M. A. Hapgood,<sup>2</sup> M. J. Owens,<sup>1</sup> C. J. Davis,<sup>1,2</sup> and F. Steinhilber<sup>3</sup>

Received 10 June 2011; revised 2 July 2011; accepted 7 July 2011; published 19 August 2011.

[1] The recent decline in the open magnetic flux of the Sun heralds the end of the Grand Solar Maximum (GSM) that has persisted throughout the space age, during which the largest-fluence Solar Energetic Particle (SEP) events have been rare and Galactic Cosmic Ray (GCR) fluxes have been relatively low. In the absence of a predictive model of the solar dynamo, we here make analogue forecasts by studying past variations of solar activity in order to evaluate how long-term change in space climate may influence the hazardous energetic particle environment of the Earth in the future. We predict the probable future variations in GCR flux, near-Earth interplanetary magnetic field (IMF), sunspot number, and the probability of large SEP events, all deduced from cosmogenic isotope abundance changes following 24 GSMs in a 9300-year record. **Citation:** Barnard, L., M. Lockwood, M. A. Hapgood, M. J. Owens, C. J. Davis, and F. Steinhilber (2011), Predicting space climate change, *Geophys. Res. Lett.*, *38*, L16103, doi:10.1029/2011GL048489.

### 1. Past Variations in Space Climate Hazards

[2] Geomagnetic activity records [Lockwood *et al.*, 1999, 2009] and abundances of cosmogenic radionuclides, generated by Galactic Cosmic Rays (GCRs) and stored in terrestrial reservoirs [Steinhilber *et al.*, 2008, 2010], have revealed and quantified centennial and millennial variations in the open solar flux and the near-Earth Interplanetary Magnetic Field (IMF), *B*. The agreement between the reconstructions is remarkable, given that the two techniques are independent [Lockwood and Owens, 2011]. The cosmogenic isotopes show that in recent decades the Sun has been in a Grand Solar Maximum (GSM) which has lasted longer than all others in the past 9.3 millennia and is expected to end soon [Abreu *et al.*, 2008]. This is supported by geomagnetic and satellite observations which show a decline in mean *B* since 1985 [Lockwood and Fröhlich, 2007; Lockwood *et al.*, 2009], of which the recent low and prolonged sunspot minimum is part [Lockwood, 2010]. These changes in near-Earth space influence the occurrence of space-weather phenomena, returning Earth to conditions that last prevailed around 1920 [Lockwood *et al.*, 2009; Steinhilber *et al.*, 2010; Lockwood and Owens, 2011], before the advent of susceptible modern operational systems, such as spacecraft,

power distribution grids and aircraft [Hapgood, 2011]. McCracken and Beer [2007] have used Monte-Carlo simulations to combine cosmogenic isotope data with observations by modern ionisation chambers and neutron monitors and shown that higher GCR intensities existed before the space age and noted that they were likely to reoccur in the future. McCracken [2007] extended the study of McCracken and Beer [2007] to high-fluence Solar Energetic Particle (SEP) events (sufficient to be seen as “Ground-Level Enhancements”, GLEs, in neutron monitor data) to demonstrate that SEPs were also more frequent in the past and deduced that their fluence was also likely to increase in future.

[3] Measurements of nitrates in ice cores has led to the identification of 15 major SEP events (fluence of >30 MeV protons exceeding  $5 \times 10^9 \text{ cm}^{-2}$ ) during 1700–1970 [Shea *et al.*, 2006] which gives an average SEP event occurrence per century of  $P_{\text{SEP}} = 5.6$  for this interval. In contrast, spacecraft measurements [Barnard and Lockwood, 2011] during 1970–2009 yield just 1 equivalent event, an occurrence of  $P_{\text{SEP}} = 2.6$  per century. This decrease was also identified in GLE events by McCracken [2007].

[4] At cruise altitudes of commercial aviation, both SEPs and GCRs pose threats through single event upsets in critical electronics and through exposure of crew and passengers to radiation [Dyer *et al.*, 2003; Barish, 2009]. Radiation standards for avionics are based on past experience from the current GSM and there are no regulations concerning passenger exposure. Allowed radiation limits on the ground vary between nations. The International Commission on Radiological Protection (ICRP) recommends a 20 mSv limit for the annual exposure of occupational radiation workers and a 1 mSv limit for the public and prenatal annual exposure [Wrixon, 2008; Mertens *et al.*, 2010]. Dosages during a flight depend on path, duration and altitude as well as solar activity. For example, Mertens *et al.* [2010] find a commercial 8-hour polar flight during the 2003 “Halloween” SEP event would have given 0.7 mSv. Models such as QARM [Lei *et al.*, 2006] (which can run be online at <http://qarm.space.qinetiq.com/>) show that a round trip of two such flights during the recent solar minimum gave a GCR dose of order 0.2 mSv and during the largest known SEP event, the “Carrington event” of 1859 [Shea *et al.*, 2006; Hapgood, 2011], would have given 20 mSv. Some flights have already been diverted to lower latitudes and altitudes based on solar event warnings (mainly to avoid communications blackouts rather than the associated SEP hazard) with monetary and flight-time costs [Fisher and Jones, 2007]. GCRs and SEPs are also a threat to spacecraft, reducing operational lifetimes and thus returns on investment. Current engineering and business models are also based on experience gained during the current GSM and long-term solar change will impact the economics of commercial space activities. Esti-

<sup>1</sup>Space Environment Physics, Department of Meteorology, University of Reading, Reading, UK.

<sup>2</sup>RAL Space, Rutherford Appleton Laboratory, Chilton, UK.

<sup>3</sup>EAWAG, Swiss Federal Institute of Aquatic Science and Technology, Dübendorf, Switzerland.

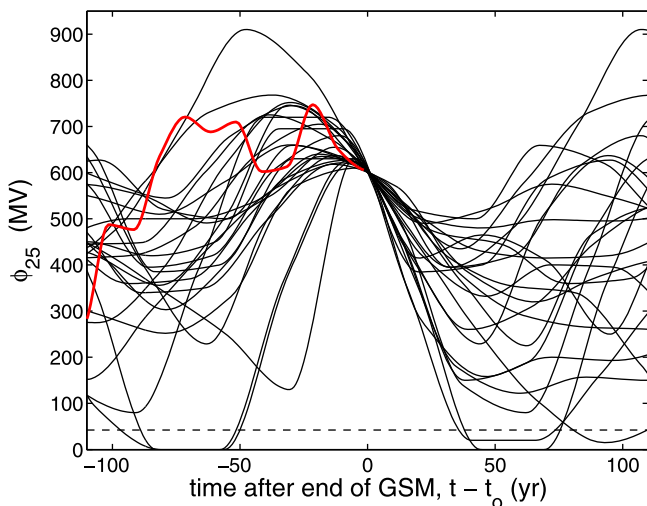


**Figure 1.** Composite of variations of annual solar modulation potential values,  $\phi_{25}$ , (interpolated from the 25-year means by *Steinhilber et al.* [2008] using cubic splines) around the 24 ends of grand solar maxima (at times  $t_0$ ) in the past 9300 years. This is an updated version of *Lockwood* [2010, Figure 6]. The times  $t_0$  are defined to be when  $\phi_{25}$  fell below the 600 MV level. The horizontal dashed line is the Maunder minimum  $\phi_{25}$  and the data for the past 110 years from the PCA analysis of *Steinhilber et al.* [2010] is shown by the red line. As 2 of the 24 cases fall below the Maunder minimum level at  $(t - t_0) < 40$  yr, this has a probability of about 8%.

mates vary, but from studies of smaller events, the direct and knock-on (loss of service etc.) costs of a Carrington-scale event have been estimated at \$1–2 trillion and full recovery would take 4–10 years [*Odenwald et al.*, 2006].

[5] To understand how solar activity may evolve in the future, we need to study past behaviour. We here use the 9300-year record of 25-year means of the solar modulation potential  $\phi$  compiled by *Steinhilber et al.* [2008] from cosmogenic isotope and neutron monitor data:  $\phi$  quantifies the solar shielding of the Earth from GCRs and taking  $\phi \geq 600$  MV defines 24 GSMs prior to the current one. *Lockwood* [2010] carried out a superposed-epoch study of  $\phi$  around the ends of these 24 GSMs (at times  $t = t_0$ ). Figure 1 is an updated version of that study and shows that the chance of 25-year running means,  $\phi_{25}$ , falling to Maunder minimum levels at  $(t - t_0) \leq 40$  years is 8%. We here take the mean  $\phi_M$  and standard deviation  $\sigma$  of the composited  $\phi_{25}$  at a given  $(t - t_0)$ , and use upper and lower values,  $\phi_U = \phi_M + 2\sigma$  and  $\phi_L = \phi_M - 2\sigma$  (exceeded in about 5 and 95% of cases, respectively) as predictions of the range of likely behaviours after the end of the current GSM.

[6] Figure 2 demonstrates how the solar cycle variations are added to the means shown in Figure 1, using the procedure developed by *Lockwood et al.* [2011] and the reconstruction of annual values of  $\phi$  by *Usoskin et al.* [2002] for 1720 onwards. The polynomial fit is used to estimate  $\phi$  for a predicted  $\phi_{25}$  and solar cycle phase,  $\varepsilon$ .

## 2. Analogue Forecasts of the Future

[7] Figure 3a shows past variations of  $\phi$  (in black) and  $\phi_{25}$  (in grey), from *Usoskin et al.* [2002] and *Steinhilber et al.* [2008] respectively, in the 110 years leading up to the end

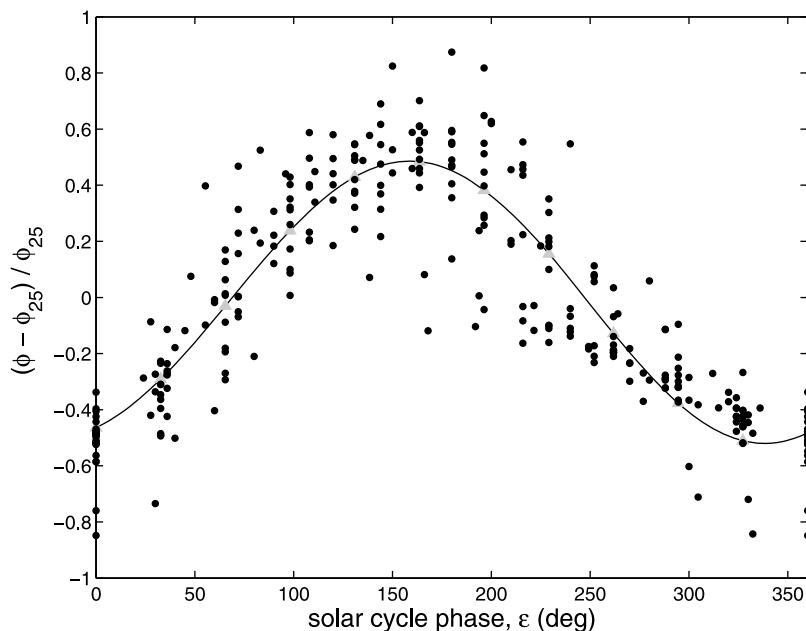


**Figure 2.** The variation of detrended annual means of the modulation potential  $\phi$  with solar cycle phase  $\varepsilon$ . The values of the fractional deviation from 25-year means  $(\phi - \phi_{25})/\phi_{25}$  are plotted where  $\phi$  are the annual values for 1720–2000 reconstructed by *Usoskin et al.* [2002] and  $\phi_{25}$  is the simultaneous value derived from the 25-year means of *Steinhilber et al.* [2008], as also shown in Figure 1. The solar cycle phase is derived from solar minimum dates in  $\phi$  using the procedure adopted by *Lockwood and Owens* [2009]. Black dots are annual values and the line is the best-fit 8th order polynomial. The grey triangles give annual fitted values, assuming the solar cycle length is 11 years.

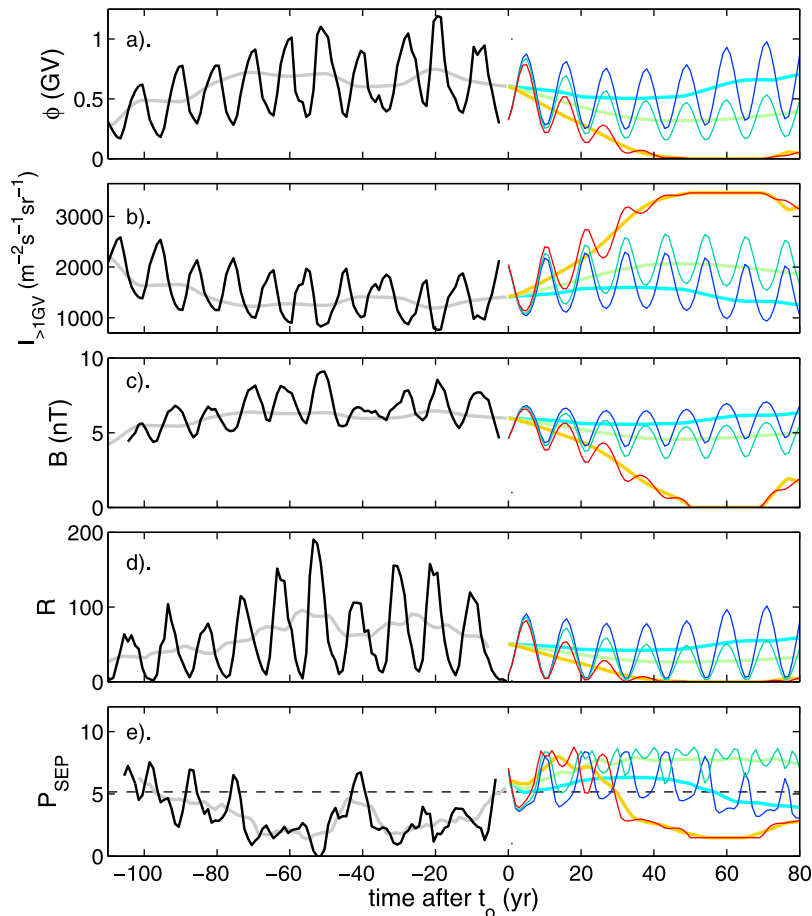


**Figure 3.** Past and future variations of (a) solar modulation potential,  $\phi$ ; (b) integral flux of galactic cosmic rays above a geomagnetic rigidity cut-off of 1 GV,  $I_{>1\text{GV}}$ ; (c) near-Earth interplanetary magnetic field,  $B$ ; (d) sunspot number,  $R$ ; and (e) the probable number of a large SEP events per century,  $P_{\text{SEP}}$ . All are shown as a function of time after  $t_0$  (when  $\phi$  falls to 600 MV). The black lines are from past observations, the grey line showing the 25-year running means. Thick cyan, green and orange lines are predicted future values for  $\phi_U$ ,  $\phi_M$  and  $\phi_L$  (see text). The blue, green and red thin lines are predicted annual values assuming all future solar cycles are 11 yrs long. The variations in Figure 3e are derived from the corresponding variations in Figures 3c and 3d using a polynomial fit to large SEP event occurrence as a function of  $B$  and  $R$  (Figure 5c) and the dashed line is the mean for 1700–2009.

of the current GSM, taken to be at  $t_0 = 2014$  [Lockwood *et al.*, 2009]. The plot also uses the composite in Figure 1 to predict  $\phi_M$ ,  $\phi_U$  and  $\phi_L$  at a given  $(t - t_0)$ , as shown by the thick green, cyan and orange lines, respectively. The annual values for these predicted 25-year means are then computed for  $t > t_0$  from the polynomial fit shown in Figure 2, where  $\varepsilon$  is computed by assuming future solar cycles are all of the average 11-year duration (shown by the thin green, blue and red lines for  $\phi_M$ ,  $\phi_U$  and  $\phi_L$ , respectively).

[8] Figure 3 also shows the corresponding plots for the integrated GCR flux for a geomagnetic rigidity cut-off of 1 GV,  $I_{>1\text{GV}}$  (Figure 3b); the IMF,  $B$  (Figure 3c) and the sunspot number  $R$  (Figure 3d). The predicted  $\phi_M$ ,  $\phi_L$ , and  $\phi_U$  are converted into the corresponding values of  $B$  and  $I_{>1\text{GV}}$ ; the former using the formula by Steinhilber *et al.* [2010], the latter by integrating the formula for differential GCR flux by Castagnoli and Lal [1980] and using their model local interstellar GCR spectrum. Note that 1 GV is used here because it applies at geomagnetic latitude of about  $60^\circ$  and so is relevant to high-latitude aircraft flights. For  $R$ ,

the conversion is made using a linear regression of 25-year means of  $R$  and  $\phi_{25}$  for 1700–2009. Once the 25-year running means of  $I_{>1\text{GV}}$ ,  $B$  and  $R$  have been computed, the solar cycle variation in annual means is constructed using the same procedure as was applied to  $\phi$  in Figure 2. A grand minimum ( $\phi$  lower than in the Maunder minimum) occurs within 40 years of  $t_0$  for  $\phi_L$ , giving near-zero  $R$  and  $B$  and with  $I_{>1\text{GV}}$  rising to 2.5 times the average for recent decades. On the other hand,  $\phi_U$  yields only a slight and brief rise in  $I_{>1\text{GV}}$  and  $\phi_M$  gives a rise by a factor near 1.5. Additionally we calculated the integrated GCR flux for the cut-off of the Climax neutron monitor (3 GV) (not shown). We find an increase in  $I_{>3\text{GV}}$  of about 40% for  $\phi_L$  which agrees well with the Maunder minimum value derived by McCracken and Beer [2007].

[9] Figures 4, 5, and 3e analyse the other energetic particle hazard, SEPs. We employ the recent survey of gradual SEPs at energies  $>60$  MeV [Barnard and Lockwood, 2011], predominantly generated at the shocks ahead of super-Alfvénic coronal mass ejections (CMEs) [Reames, 2004].

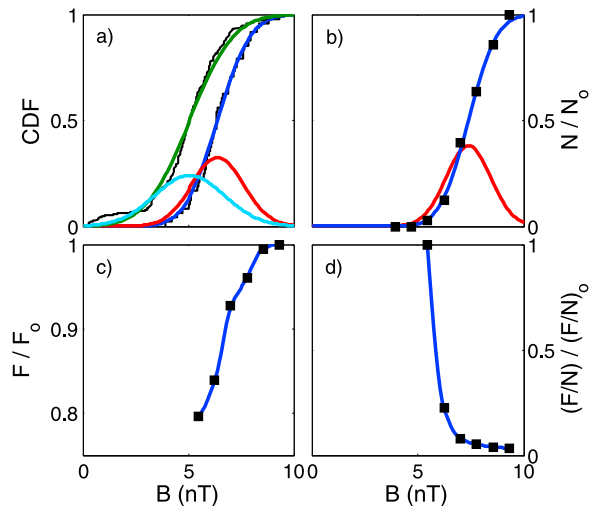


**Figure 4.** Analysis of the occurrence and fluence of gradual SEP events from a survey of space-age data [Barnard and Lockwood, 2011]. (a) The Cumulative Distribution Functions (CDF) of annual  $B$  values for 1968–2009 and 1700–2009, which are fitted with Gaussian distributions to give the blue and green lines, respectively. The red and cyan lines give the corresponding Probability Density Functions (PDFs). The other three panels are for data from 1968–2009 only and show the results for all  $B$  below threshold values given by the x axis. (b) The number of SEPs as a ratio of the total number  $N_0$ , the red line showing that the corresponding PDF is quite similar to, but somewhat narrower than, that of  $B$  for the same interval (shown in red in a). (c) The logarithm of integrated event fluence,  $F$ , as a ratio of the corresponding value for all events,  $F_0$ . (d) The normalized log fluence per event  $(F/N)/(F/N)_0$ .

Figure 4a shows the probability distributions of annual means of measured and reconstructed  $B$  for 1968–2009 and 1700–2009, respectively. It can be seen that  $B$  in the space age has been higher (because it is within the recent GSM). Figure 4b shows the fraction of SEP events,  $N/N_0$ , at  $B$  below the threshold given by the x-axis and 4c shows the corresponding normalised logarithm of the integrated fluence in those events,  $F/F_0$  ( $N_0$  is the total number of events and  $F_0$  is the logarithm of the integrated total fluence). Both decrease as the  $B$  reduces, but  $N/N_0$  falls more rapidly than  $F/F_0$  so the log of the fluence per event,  $(F/N)$  increases rapidly (Figure 4d). This shows that although SEP events become rarer as  $B$  decreases, the mean fluence within each event increases dramatically. This agrees with the analysis of GLE event occurrence by McCracken [2007].

[10] Figures 5a and 5b compare the intervals 1700–2009 and 1968–2009. The contours give the number of years with mean  $B$  falling in bins 1nT wide and with mean  $R$  in bins of width 25. In both plots, the black dots are the large SEP events (fluence of 30 MeV protons  $>5 \times 10^9 \text{cm}^{-2}$ ) as inferred from nitrates deposited in ice sheets [McCracken et al., 2001; Shea et al., 2006] and as directly measured by spacecraft. The radius of the dot is proportional to the log of the event fluence. Note that the events define a band at intermediate  $B$  values and that they cluster around a  $B$  which increases with  $R$ . It has been postulated [McCracken et al., 2001] that when  $B$  is low, the occurrence of large and fast CMEs is also low but that at large  $B$  the consequent enhanced Alfvén speed of the interplanetary medium reduces the CME shock compression ratio and hence the efficiency of SEP acceleration. Combined, these two factors could therefore explain why large events are more common in a band at intermediate  $B$ . The open flux continuity equation [Vieira and Solanki, 2010] has a production term that depends on  $R$  and CME rate and a loss term which depends on other factors such as the heliospheric current sheet tilt [Owens et al.,

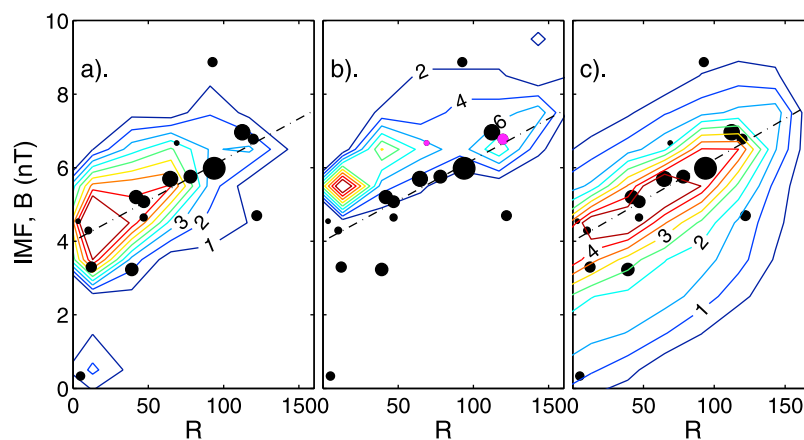


**Figure 5.** Black dots are plotted at the annual means of sunspot number,  $R$ , and IMF,  $B$ , of major SEP events (fluence of 30 MeV protons  $>5 \times 10^9 \text{cm}^{-2}$ ) during 1700–2009 [Shea et al., 2006]: the size of each dot is proportional to the log of the estimated event fluence. The contours in Figures 5a and 5b are the percent of years when the annual means of  $R$  and  $B$  fall into bins that are 25 and 1nT wide, respectively: (a) all years after the Maunder minimum (1700–2009); (b) the space age (1968–2009). The  $B$  values in Figure 5a are from geomagnetic data [Lockwood et al., 2009] extended back to 1700 using modelled open solar flux [Vieira and Solanki, 2010] and converted into  $B$  using a polynomial fit [Lockwood and Owens, 2011]. In Figure 5b observed  $B$  are used and the large SEPs in this interval are colored mauve. The dashed line is the linear regression fit to the event coordinates. (c) Contours of  $P_{\text{SEP}}$  derived by taking the PDFs of event occurrence with distances along and perpendicular to the dashed regression line.

2011]; as a result, although  $B$  increases with  $R$  on average, a spread of  $B$ - $R$  combinations is possible. Figure 5b shows that in the space age,  $B$  has generally been higher than the optimum combination of  $B$  and  $R$  for large SEPs to occur. This contrasts with Figure 5a in which optimum combinations were much more common. Figure 5c shows contours of the SEP rate  $P_{\text{SEP}}$  as a function of  $R$  and  $B$ , derived from a fit to the occurrence frequency of all events. Annual ( $B$ ,  $R$ ) coordinates vary both over solar cycles and on longer timescales and it is found that they often move in and out of the band of high  $P_{\text{SEP}}$  occurrence at varying phases of the cycle.

[11] Figure 3e shows  $P_{\text{SEP}}$  variations derived from the annual  $R$  and  $B$  means using Figure 5c. During the recent solar minimum the fall in  $B$  caused  $P_{\text{SEP}}$  to rise. For predictions based on  $\phi_L$ , the average probability of a large event continues to rise (by to up to 3 times) before falling to low values as the Sun enters the grand minimum. For  $\phi_U$ ,  $P_{\text{SEP}}$  shows oscillations similar to the present solar cycle before a slow decay: peak  $P_{\text{SEP}}$  occur for the lower  $B$  values at sunspot minimum, as was true for the interval 1900–1930 ( $-102 < t - t_0 < -72$  yr). The most likely exit from the current GSM is given by  $\phi_M$  which yields persistently higher  $P_{\text{SEP}}$  than we have experienced during the current GSM. The solar cycle variation is different to the other two cases, showing lowest  $P_{\text{SEP}}$  at sunspot minima with clear peaks in both the rising and falling phases: the average  $P_{\text{SEP}}$  remains enhanced throughout the next century.

[12] This analysis reveals that the risk of the space-weather radiation effects is considerably enhanced over the next century compared to the space age thus far. There is an 8% chance of the Sun falling into a grand minimum during the next 40 years [Lockwood, 2010], giving enhanced dosages of GCR radiation which is of concern for aircraft avionics, crew and passengers. The risk of large SEP events is initially enhanced in this case but then is low during the grand minimum itself. A more likely scenario is given by the mean of all previous examples and this predicts a more modest rise in the GCR fluxes but a persistently enhanced risk of a large SEP event. Lastly we note that both GCR and SEP enhancements will be amplified by the probable continuation of the decrease in the geomagnetic field, and the shielding it provides, that has been observed over the past 160 years [Gubbins et al., 2006].

[13] **Acknowledgments.** L.B. was supported by a Ph.D. studentship from the UK Natural Environment Research Council, M.L., M.A.H. and C.J.D. are funded by the Science and Technology Research Council and FS by NCCR climate (Swiss climate research).

[14] The Editor thanks Margaret Shea and an anonymous reviewer for their assistance in evaluating this paper.

## References

- Abreu, J. A., J. Beer, F. Steinhilber, S. M. Tobias, and N. O. Weiss (2008), For how long will the current grand maximum of solar activity persist?, *Geophys. Res. Lett.*, *35*, L20109, doi:10.1029/2008GL035442.
- Barish, R. J. (2009), Health physics and aviation: solar cycle 23 (1996–2008), *Health Phys.*, *96*(4), 456–464, doi:10.1097/01.HP.0000338338.71484.3c.
- Barnard, L., and M. Lockwood (2011), A survey of gradual solar energetic particle events, *J. Geophys. Res.*, *116*, A05103, doi:10.1029/2010JA016133.
- Castagnoli, G., and D. Lal (1980), Solar modulation effects in terrestrial production of carbon-14, *Radiocarbon*, *22*(2), 133–158.
- Dyer, C. S., F. Lei, S. N. Clucas, D. F. Smart, and M. A. Shea (2003), Calculations and observations of solar particle enhancements to the radiation environment at aircraft altitudes, *Adv. Space Res.*, *32*, 81–93, doi:10.1016/S0273-1177(03)90374-7.
- Fisher, G., and B. Jones (2007), Meeting report: Integrating space weather observations and forecasts into aviation operations, *Space Weather*, *5*, S07003, doi:10.1029/2007SW000328.
- Gubbins, D., A. L. Jones, and C. C. Finlay (2006), Fall in Earth's magnetic field is erratic, *Science*, *312*, 900–902, doi:10.1126/science.1124855.
- Hapgood, M. A. (2011), Towards a scientific understanding of the risk from extreme space weather, *Adv. Space Res.*, *47*, 2059–2072, doi:10.1016/j.asr.2010.02.007.
- Lei, F., A. Hands, S. Clucas, C. Dyer, and P. Truscott (2006), Improvement to and Validations of the QinetiQ Atmospheric Radiation Model (QARM), *IEEE Trans. Nucl. Sci.*, *53*(4), 1851–1858, doi:10.1109/TNS.2006.880567.
- Lockwood, M. (2010), Solar change and climate: an update in the light of the current exceptional solar minimum, *Proc. R. Soc. A*, *466*, 303–329, doi:10.1098/rspa.2009.0519.
- Lockwood, M., and C. Fröhlich (2007), Recent oppositely directed trends in solar climate forcings and the global mean surface air temperature, *Proc. R. Soc. A*, *463*, 2447–2460, doi:10.1098/rspa.2007.1880.
- Lockwood, M., and M. J. Owens (2009), The accuracy of using the Ulysses result of the spatial invariance of the radial heliospheric field to compute the open solar flux, *Astrophys. J.*, *701*(2), 964–973, doi:10.1088/0004-637X/701/2/964.
- Lockwood, M., and M. J. Owens (2011), Centennial changes in the heliospheric magnetic field and open solar flux: The consensus view from geomagnetic data and cosmogenic isotopes and its implications, *J. Geophys. Res.*, *116*, A04109, doi:10.1029/2010JA016220.
- Lockwood, M., R. Stamper, and M. N. Wild (1999), A doubling of the Sun's coronal magnetic field during the last 100 years, *Nature*, *399*, 437–439, doi:10.1038/20867.
- Lockwood, M., A. P. Rouillard, and I. D. Finch (2009), The rise and fall of open solar flux during the current grand solar maximum, *Astrophys. J.*, *700*(2), 937–944, doi:10.1088/0004-637X/700/2/937.
- Lockwood, M., R. G. Harrison, M. J. Owens, L. Barnard, T. Woollings, and F. Steinhilber (2011), The solar influence on the probability of relatively cold UK winters in the future, *Environ. Res. Lett.*, *6*, 034004, doi:10.1088/1748-9326/6/3/034004.
- McCracken, K. G. (2007), High frequency of occurrence of large solar energetic particle events prior to 1958 and a possible repetition in the near future, *Space Weather*, *5*, S07004, doi:10.1029/2006SW000295.
- McCracken, K. G., and J. Beer (2007), Long term changes in the cosmic ray intensity at Earth, 1428–2005, *J. Geophys. Res.*, *112*, A10101, doi:10.1029/2006JA012117.
- McCracken, K. G., G. A. M. Dreschhoff, E. J. Zeller, D. F. Smart, and M. A. Shea (2001), Solar cosmic ray events for the period 1561–1994: 1. Identification in polar ice 1561–1950, *J. Geophys. Res.*, *106*, 21,585–21,598, doi:10.1029/2000JA000237.
- Mertens, C. J., B. T. Kress, M. Wiltberger, S. R. Blattnig, T. S. Slaba, S. C. Solomon, and M. Engel (2010), Geomagnetic influence on aircraft radiation exposure during a solar energetic particle event in October 2003, *Space Weather*, *8*, S03006, doi:10.1029/2009SW000487.
- Odenwald, S. F., J. L. Green, and W. Taylor (2006), Forecasting the impact of an 1859-calibre superstorm on satellite resources, *Adv. Space Res.*, *38*(2), 280–297, doi:10.1016/j.asr.2005.10.046.
- Owens, M. J., N. U. Crooker, and M. Lockwood (2011), How is open solar magnetic flux lost over the solar cycle? *J. Geophys. Res.*, *116*, A04111, doi:10.1029/2010JA016039.
- Reames, D. V. (2004), Solar energetic particle variations, *Adv. Space Res.*, *34*(2), 381–390, doi:10.1016/j.asr.2003.02.046.
- Shea, M. A., D. F. Smart, K. G. McCracken, G. A. M. Dreschhoff, and H. E. Spence (2006), Solar proton events for 450 years: The Carrington event in perspective, *Adv. Space Res.*, *38*(2), 232–238, doi:10.1016/j.asr.2005.02.100.
- Steinhilber, F., J. A. Abreu, and J. Beer (2008), Solar modulation during the Holocene, *Astrophys. Space Sci. Trans.*, *4*, 1–6, doi:10.5194/astr4-1-2008.
- Steinhilber, F., J. A. Abreu, J. Beer, and K. G. McCracken (2010), Interplanetary magnetic field during the past 9300 years inferred from cosmogenic radionuclides, *J. Geophys. Res.*, *115*, A01104, doi:10.1029/2009JA014193.
- Usoskin, I. G., K. Mursula, S. K. Solanki, M. Schüssler, and G. A. Kovaltsov (2002), A physical reconstruction of cosmic ray intensity since 1610, *J. Geophys. Res.*, *107*(A11), 1374, doi:10.1029/2002JA009343.

Vieira, L. E. A., and S. K. Solanki (2010), Evolution of the solar magnetic flux on time scales of years to millennia, *Astron. Astrophys.*, 509, A100, doi:10.1051/0004-6361/200913276.

Wrixon, A. D. (2008), New ICRP recommendations, *J. Radiol. Protect.*, 28, 161–168, doi:10.1088/0952-4746/28/2/R02.

---

L. Barnard, C. J. Davis, M. Lockwood, and M. J. Owens, Space Environment Physics, Department of Meteorology, University of Reading,

Earley Gate, PO Box 243, Reading RG6 6BB, UK. (m.lockwood@reading.ac.uk)

M. A. Hapgood, RAL Space, Rutherford Appleton Laboratory, Harwell Campus, Chilton, Didcot, Oxfordshire OX11 0QX, UK.

F. Steinhilber, EAWAG, Swiss Federal Institute of Aquatic Science and Technology, PO Box 611, Ueberlandstr. 133, CH-8600 Dübendorf, Switzerland.